Multi-modal and multi-layer robustness analysis of the European rail and air networks

Ippolito, Nicola; Cats, Oded

DOI
10.1038/s41598-024-76264-6

Publication date
2024

Document Version
Final published version

Published in
Scientific Reports

scientific reports

Check for updates

OPEN

Multi-modal and multi-layer robustness analysis of the European rail and air networks

Nicola Ippolito[1] & Oded Cats[2]✉

The robustness of long-distance transport services is paramount for ensuring network connectivity under disruptions. We conduct a comparative analysis of the European rail and air networks of 124 main metropolitan areas, assessing their ability to withstand successive network degradation. We undertake a multi-modal and multi-layer approach in our analysis of the robustness of long-distance transport networks. In particular, we are interested in the role of individual nodes for both air and rail networks as well as for the integrated multi-modal network. Given the hierarchical nature of long-distance transport services, we adopt a multi-layer perspective by means of clustering nodes based on their criticality in order to identify common performance profiles. Original metrics are formulated to measure the impact of nodes on network fragmentation, both at the individual level and as cluster members. Additionally, a new metric is introduced to assess cities' reliance on air transportation, when considering the integrated multi-layer air-rail network during disruptions in air connections. Our findings indicate that the air network exhibits significantly greater robustness compared to rail, i.e. 10% versus 71% performance loss in the worst case scenario, respectively. Furthermore, primary sub-graph of nodes whose protection from attacks can greatly enhance network's overall robustness is identified. We discuss our findings in terms of the relationship between network structure, robustness, and the role of critical nodes as well as propose potential mitigation measures.

Keywords Network robustness, Targeted and random failures, Rail and air networks

The development of complex transportation networks and their indispensable role in providing essential services have underscored the significance of studying their robustness in recent decades. Transportation systems are subject to recurrent disruptions which result with their partial degradation[1]. While the related notions of network vulnerability allows for multiple interpretations[2], network robustness is widely defined as network's ability to withstand or absorb disturbances and remain intact when exposed to disruptions[3]. These disruptions can be categorized as either internal or external events, and accidental or intentional[4], such as mechanical failures (internal and accidental events), or deliberate attacks (external and intentional events). Past works in the field of transport network robustness can be classified into one of the following key threads: mathematical modeling to identify critical network elements[5–7], and frameworks and metrics for evaluating network robustness[8–12]. Our work contributes to both threads.

The aim of this study is to comprehensively analyze and compare the robustness of the European air and rail networks and quantify node criticality therein. In the aviation context, a distinction can be made amongst studies focusing on global or regional networks, airline alliances and individual airlines and airports[13]. Within the former category, several studies have used network science indicators to investigate the structure and measure the robustness of the European[14], Chinese[15], US[16] or global[17] airline networks. Similarly, the topological characteristics and the hierarchical structure of high-speed rail were investigated[18,19] as well as its network robustness[20]. In the case of high-speed rail, all of the aforementioned studies have considered the Chinese network in their analysis.

Our study focuses on the long-distance transport system by quantifying and comparing the robustness of the air and rail networks as well as by investigating the multi-modal network resulting from the integration of the air and rail sub-networks. To the best of our knowledge, only a couple of studies have specifically investigated the interaction between the robustness of the air and high-speed rail networks. These pioneering studies have quantified the complementary effect of high-speed rail networks for the robustness of the air network[21] and measured the robustness of the coupled network in terms of the impact of disruptions on link capacity

[1]DICEA, Sapienza University of Rome, Rome, Italy. [2]Department of Transport and Planning, Delft University of Technology, Delft, The Netherlands. ✉email: o.cats@tudelft.nl

utilisation[22]. Both studies performed their analysis for the Chinese air and high-speed rail networks in relation to successive network degradation scenarios.

We undertake a multi-modal and multi-layer approach in our analysis of the robustness of long-distance transport networks. In particular, we are interested in the role of individual nodes for both air and rail networks as well as for the integrated multi-modal network. To this end, we propose new metrics for quantifying the roles of individual nodes in contributing to network degradation. Given the hierarchical nature of long-distance transport services, we adopt a multi-layer perspective by means of clustering nodes based on their criticality in order to identify common performance profiles. Our European network consists of 124 nodes corresponding to key metropolitan areas located in 34 European countries, enabling a consistent and comparable representation for comparing the performance of air and rail networks. In addition, we examine the added-value of an integration between rail and air transport for the multi-modal and multi-layer European long-distance network robustness. Figure 1 offers a schematic presentation of the adopted methodology, consisting of an algorithmic flow (left) and output analysis (right). Our node failing algorithm is a degeneration process which iteratively removes nodes from the network, and terminates when all nodes have been removed.

Results

Comparison of rail network and air network robustness

We investigate the robustness of the network by testing for its ability to function under an iterative procedure which removes each time one node[17,23,24] $(i \in N)$ and all edges targeting to or sourcing from it $(e \in E)$ from the graph $G(N, E)$. All nodes are successively selected according to strategy σ and removed. The strategy defines the sequence of failed nodes, where each entry corresponds to the removed node $s^{(k)} \in N^{(k)}$ at stage $k+1$. Index k ranges from 0 to $|N|-1$, and the failure sequence has length $|N|-2$ since removal is at the successive stage. The largest connected component is adopted as a metric for measuring the remaining network functionality[17,25,26] denominated by $L(x)$, where x is the fraction of removed nodes. Strategies intend to either mimic *targeted*

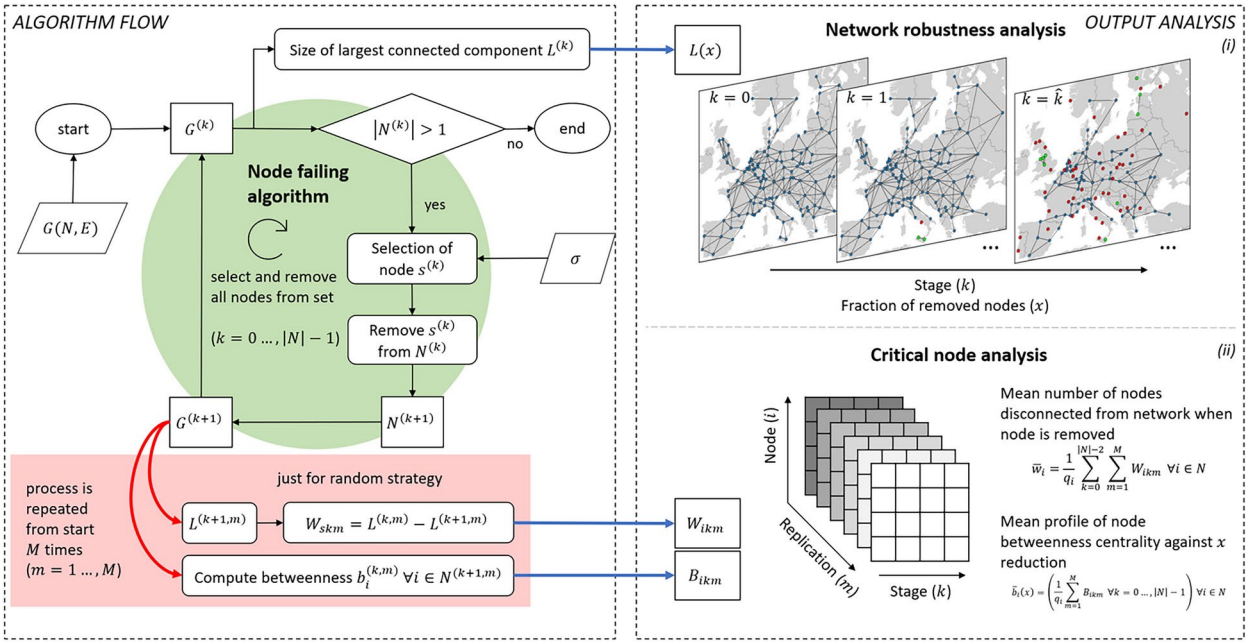

Fig. 1. Framework for network robustness and critical nodes analysis. The directed graph $G(N, E)$, with sets of nodes N and edges E, serves as the input. Node failing algorithm (green circle) is simulating the successive removal of nodes and thereby generates results for addressing both analyses. Process stages are denoted with index k. In each stage but last, a node $s^{(k)}$ is selected for removal based on a specified strategy σ (input). Subsequently, the network is updated, and the loop is repeated. If the selection process is random, the process is repeated over a specified number of replications M, so index m is used. To assess network robustness, we consider the largest connected component L for any fraction of removed nodes x. The top-right section illustrates the process for the rail network. Aligned maps depict the process of node removal, starting from a network where all nodes are active and connected (blue nodes) with corresponding infrastructure links. Moving over k indices, a node is selected for removal (depicted in red on the map). Disrupting a node renders all connected edges unavailable, potentially leading to the disconnection of other nodes (depicted in green on the map). The largest connected component L categorizes nodes as connected or disconnected. The bottom-right section pertains to the critical node analysis. This analysis is performed for the random removal strategy. Data for this analysis include the number of nodes disconnected from the network when node $s^{(k,m)}$ is removed, along with the node betweenness centrality for each node. The outcomes of the critical node analysis are organized by node, stage, and replication, resulting in three-dimensional matrices. (Maps are created using Matplotlib and Basemap https://matplotlib.org/basemap/stable/).

attacks[26] or *random failures*[27]. In the following, we investigate both and examine two types of targeted attacks: σ_d , considering the node with the highest degree $d^{(k)}$ (the number of nodes directly connected to a node at stage k) and σ_b considering the node with the highest betweenness centrality $b^{(k)}$ (the share of shortest paths that traverse a node at stage k). Due to the inherent randomness in the random removal strategy σ_r (i.e. due to path dependency), the failing process has been repeated over a number of replications M to guarantee that results are statistically robust. Hence, a series of replications $m = 1..., M$ is undertaken, where M is found[28] to be equal to 20 and 250, for the European air and rail networks, respectively. Consequently, the random removal strategy results are represented using both the sample space and the mean trend line in all subsequent plots.

We follow the aforementioned procedure in performing the robustness analyses for the European Rail and Air networks, and the results thereof are presented in Fig. 2. As can be observed by analyzing plots 2a and 2b, there are considerable differences between how the two networks perform under a sequence of node failures. First, the rail network proves less robust, arguably due to its lower connectivity (and thereby redundancy), suggesting the presence of a set of key nodes through which sub-graphs are connected to each other. In contrast, the air network proves very robust, closely following the straight descending line that corresponds to the upper bound limit. This limit reflects the scenario where the removal of each node does not lead to disconnecting any other node from the network - i.e., L is strictly equal to $|N| - k$, and all remaining nodes are connected to each other. The aggregated metric I is used to measure network robustness by calculating the area under curves[25], later normalized considering the area under the upper bound limit line: the closer I to unity, the more robust the network is in relation to the respective strategy. While under the random removal strategy $I(\sigma_r)$ results in an average of 30% performance loss for the European rail network. In the case of the European air network, the damage does not lead to any additional degradation, and each failure is limited to the attacked nodes. Second, the span of $L(x, \sigma_r)$, i.e. the range of values obtained under all random replications, is significantly different for the two networks: the range of values obtained in different replications is larger in the case of the rail network, implying a greater path-dependency in how the network performs when encountering various disruptions. Third, in the event of either type of targeted attacks, the rail network degrades rapidly, and the size of L approaches zero already when 40% of nodes are removed. The air network in contrast follows the ideal degradation trajectory until 50% of the nodes have been removed. Thereafter, the removal of nodes starts to significantly reduce L, and both targeted strategies almost fully degrade the network when almost only 20% of initial nodes remain. For European rail network, σ_b results in the fastest degradation. This suggests that there exists a set of nodes (slightly more than 10%, since for $x = 0.1$ the size of L abruptly drops) that are traversed by many of the shortest paths connecting origin-destination pairs. These nodes are central for the connections of the entire network, yielding

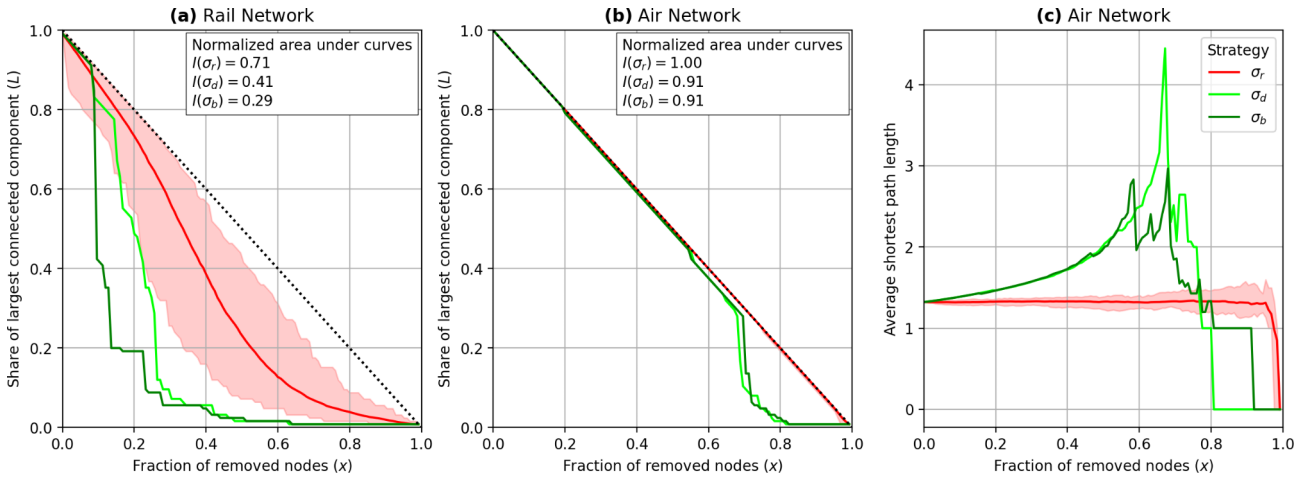

Fig. 2. The European Rail **a** and Air **b** network robustness analysis, measured in terms of the size of the largest connected component L against the fraction of removed nodes x. Solid lines correspond to the different strategies for node selection adopted in the node failing algorithm: light green σ_d and dark green σ_b correspond to targeted attack strategies - where nodes are selected according to topological score - based on either node degree or node betweenness centrality, respectively; the red line σ_r corresponds to a random failure scenario (nodes are removed in random order). The red area depicts the sample space generated across all performed replications. The dashed black diagonal serves as the upper bound limit, representing the ideal network scenario where $L(x)$ consistently matches the remaining network graph (all non-failed nodes constitute a single connected graph). The integral of the latter is used as a scale factor normalizing the area under the curves, and the values of which are reported in the top-right corner of each sub-figure. The higher the value of $I(\sigma)$, the more robust the network is to the respective node failing process. Analyzing the strategies, targeted ones yield a faster drop for both networks, suggesting that they are more efficient in causing network degradation than σ_r.Comparing the two networks, the rail network exhibits a less robust behavior, as indicated by its consistently higher distance from the upper bound limit across all strategies as compared to those obtained for the air network. The random failure scenario proves remarkably robust also in terms of the average shortest path - which corresponds here to the number of trip legs - in the Air Network (**c**) as node removal does not systematically lead to longer shortest paths amongst the remaining nodes.

an aggregate performance metric reduction of 71% when removing nodes based on their betweenness centrality value (i.e., since the normalized area under the curve when applying this removal strategy amounts to 0.29). Meanwhile, the structure of European air network renders the differences between targeted strategies remarkably small, with the total loss of aggregate performance I of no more than 10%. While the size of the largest connected component remains remarkably stable until 50% of the nodes have been removed, its functionality is impacted especially when targeted attacks are performed (2c). We find that the average shortest path increases slowly with the removal of nodes based on either node degree or node betweenness centrality up to the point at which approximately 50% of the airports have been removed, resulting in the average shortest path consisting of two legs. Beyond this point, there is a sharp increase in the average number of legs needed when travelling between airport pairs within the largest connected component, exceeding four (i.e., three transfers) when removing 70% of the airports based on their degree ranking. Subsequently, the average shortest path falls dramatically due to the collapse of the network and its fragmentation. In contrast, the random failure scenario proves remarkably robust as node removal does not systematically lead to longer shortest paths amongst the remaining nodes.

The identification of a significant path dependency when successively removing nodes from the European rail network has prompted us to further investigate its node criticality. The analysis detailed in the following section is designed to enhance our understanding of the roles and interactions of nodes in withstanding the process of network degradation.

Analyzing node criticality

Criticality analysis of individual nodes

Next, we examine the role of individual nodes - cities and their corresponding train stations - in contributing to network degradation in the event that they are disrupted and become dysfunctional. Since a node's removal impact depends on the current network state (i.e., the current set of nodes and edges), input data for this analysis are generated at each stage of each replication of the random removal strategy. Each time node i is selected to be removed, i.e. $i = s^{(k,m)}$, the extent to which the size of the largest connected component is impacted, is measured and stored, thereby allowing to quantify and compare the extent to which node's failure is detrimental to the network as a whole. This process is carried out to gather information on the mean damage that node i inflicts on the network when disrupted, denoting this metric as *mean node dependency degree*, $\bar{w}_i$. The mean node dependency degree is hence a statistical metric of the global network degradation that can be attributed to the failure of node i. Depending on the value of $\bar{w}_i$ nodes can be categorized as either connected (if its value is higher than 1) or dependent (otherwise). In the scenario where a connecting node collapses neighbors are disconnected from L as they were dependent on it to maintain their connections. When the metric equals 1 it means that on average a node failure reduced L only by its own removal. In this way the dependency of nodes on their close neighbours is explained. Figure 3 displays the $\bar{w}_i$ value for each of the nodes of the rail network. Inspecting the map (left), depicted blue nodes (ranging from dark to light blue) record $\bar{w}_i < 1$, while red nodes (ranging from light to dark red) correspond to the reversed condition. Thereby, the size of L is likely large when connecting nodes are disrupted, and almost marginal or not affected when dependent nodes fail.

The proposed indicator allows critical nodes to be identified based on the damage their removal inflicts on the rest of the network under various degradation circumstances. For example, Lille (FR), Munich (DE), and

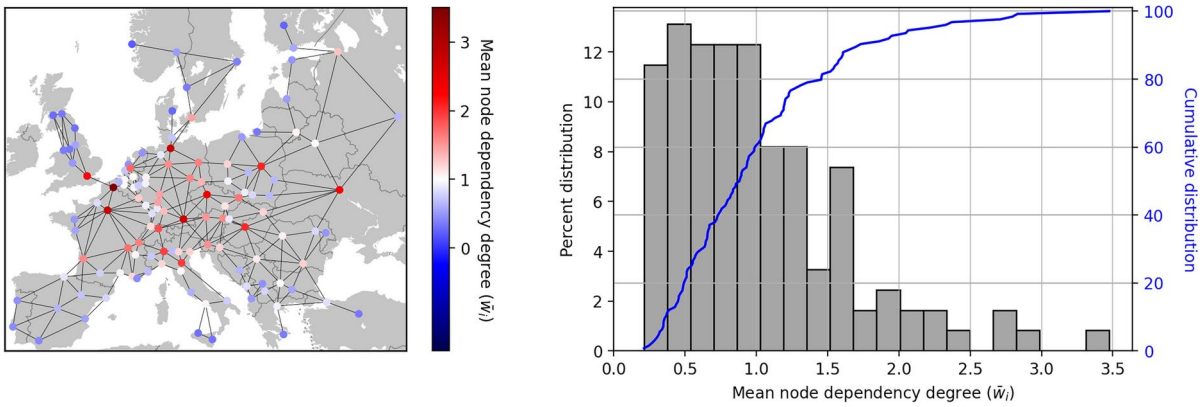

Fig. 3. Distribution of mean node dependency degree $\bar{w}_i$ for the European rail network in geographical (left) and histogram (right) plots. Mean node dependency degree is an absolute value representing how many nodes are on average becoming disconnected from the network's largest connected component when a given node is removed. Light nodes have $\bar{w}_i$ close to unity, indicating that the failure of these nodes does not lead to the isolation of additional nodes. Blue nodes have a mean dependency degree below unity, meaning that they are likely to be disconnected from the network's largest connected component following the removal of another node (referred to as dependent nodes). Conversely, red nodes are those that likely disconnect other nodes from the network's largest connected component (referred to as connecting nodes). The histogram reports the percent distribution and the cumulative distribution. Almost 60% of network nodes have a $\bar{w}_i$ lower than unity, and the 90th percentile equals 1.8. (Map is created using Matplotlib and Basemap https://matplotlib.org/basemap/stable/).

Paris (FR) record $\bar{w}_i$ values of 3.5, 2.8, and 2.7, respectively, whereas peripheral nodes such as Bergen (NO), Tampere (FI), and Glasgow (UK) exhibit the lowest values of $\bar{w}_i$, with values of 0.22, 0.27, and 0.28 respectively. The values of the latter group imply that they often become disconnected from the largest connected component as a consequence of another node being removed (this group almost counts 60% of the node set). It is possible to discern a pattern that dependent nodes are peripheral at the network's edge, while connecting nodes are more central at either geographical terms or because they are located at infrastructure bottlenecks (e.g., Lille (FR) and London (UK), serving as the only link between the European continent and the island of Great Britain). Notwithstanding, it is important to note that some geographically central nodes are not connected nodes because dense clusters of nodes provide redundant connections, allowing for bypassing node failure - i.e., the existence of cycles which allow for mitigating the impact of single node removals until reaching a critical point beyond which the network collapses. This observation highlights the importance of studying not only the role of individual nodes but also the impacts of the removal of a group of nodes in order to gain a deeper understanding of the overall robustness of the network.

Criticality analysis of clustered nodes

We seek to identify sub-sets of nodes ($C \subset N$) that respond similarly to network degradation. To this end, we cluster our nodes based on their *betweenness mean node profiles* against *x*. The betweenness centrality coefficient of each node might change whenever the network is degraded, resulting in a mean node profile over all the replications (example shown on the left side of Fig. 4 for the node of Paris).

We chose the betweenness centrality coefficient because it captures global changes in influence caused by failures which may not directly target immediate neighbors. The right side of Fig. 4 illustrates the outcome of the clustering process, revealing three distinctive clusters (C1, C2 and C3) of nodes characterized by similar trends in relation to variable *x*. The network degradation process included a constraint prohibiting the disruption of nodes within the cluster from been tested. It is important to note that for each cluster, the node failure algorithm ended only when the network exclusively comprised the nodes within the tested cluster. The node removal algorithm was executed for each cluster 250 time to reduce the effect of stochasticity in node selection. The network's resilience, considering the clusters, is depicted in Fig. 5. The three identified clusters performed as follows: C1 (orange dots in the map on the left and orange line in the plot on the right), C2 (blue), and C3 (cyan) are composed of 14%, 27%, and 59% of all network nodes. The values of the aforementioned aggregated metric can be compared to the case without cluster in plot Fig. 2a, demonstrating that introducing constraints on nodes of C1 and C2 results in robustness benefits, but not on C3 (the cyan curve shows a faster degradation process compared to the case without any constrained nodes). Specifically, the aggregate performance metric value shows that ensuring the functionality of nodes in cluster C1 or C2 improves overall network robustness to

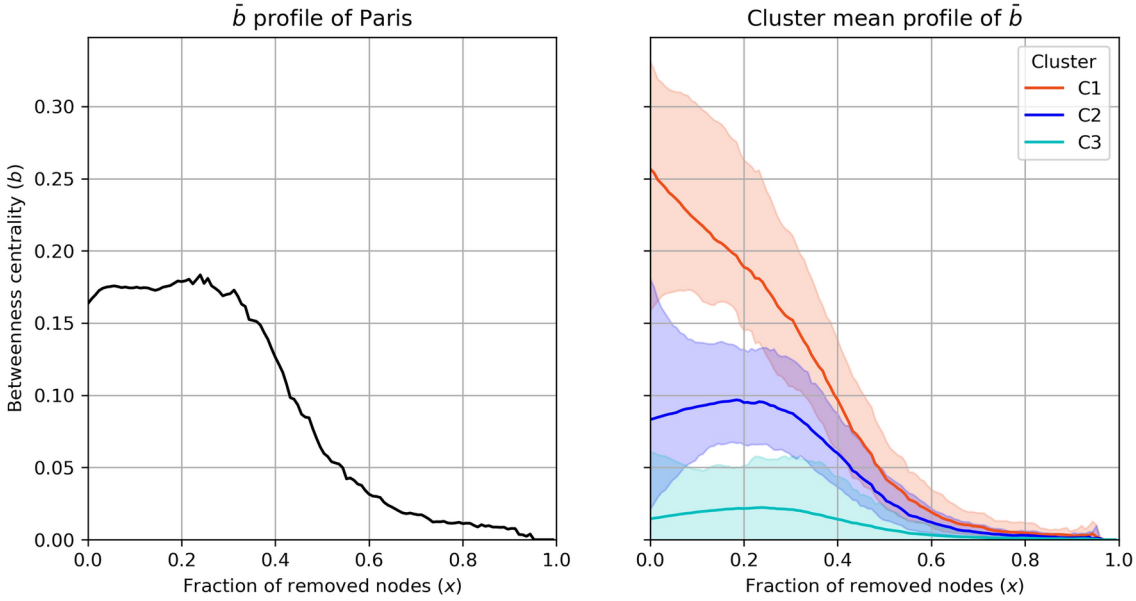

Fig. 4. The mean profile of the betweenness centrality (*b*) for the single node of Paris (left) and aggregated by clusters of nodes (right) is presented. The profile for the Paris node shows that this coefficient is an indicator representing the role of the node within the network as a whole. As can be seen, the metric varies even in response to attacks that are not in the immediate vicinity of Paris. The clusters were generated using the profiles of all nodes, and the main identified patterns are three. C1 (orange) represents the cluster of nodes with higher initial *b* values, which are immediately impacted by network reduction. C2 (blue) displays an initial increase in *b* followed by a decline to zero. This suggests that nodes in this cluster compensate for the network reduction initially, but their betweenness decreases as *x* reaches 20 to 30%. C3 (cyan) consists of nodes at the periphery of the network, showing a nearly constant behavior with *b* values close to zero across all *x* values. For the three clusters, distinct breaking points are observed, where the drop in *b* begins at different values of *x*.

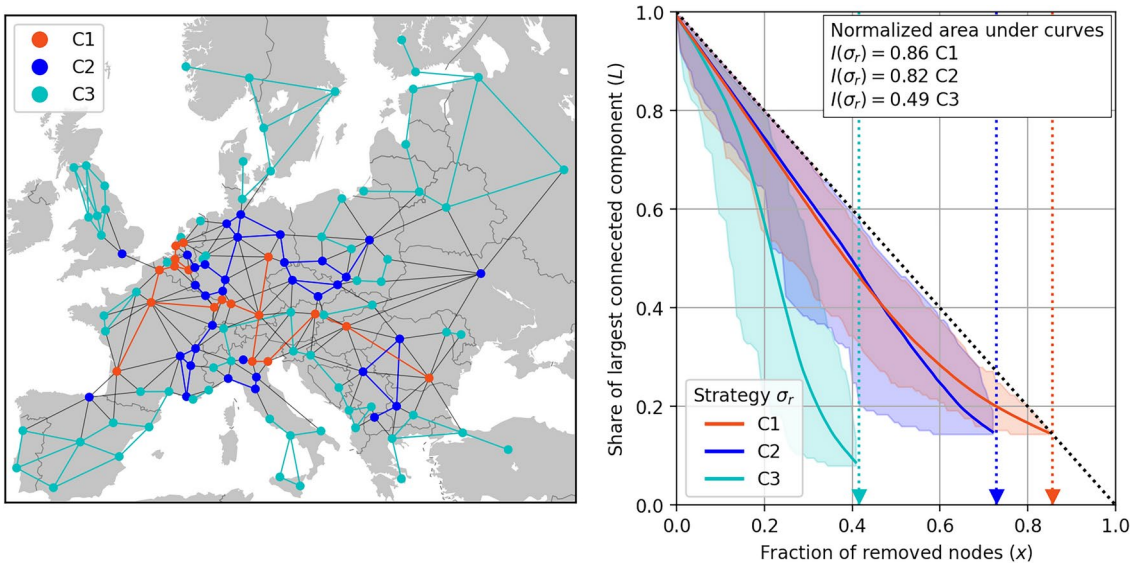

Fig. 5. Clusters of nodes with a similar mean node betweenness centrality profile in the European rail network. Three clusters are identified, C1 (orange), C2 (blue) and C3 (cyan), and their node members are shown on the map (left). Edges are depicted either in black or colored, depending on whether they connect nodes which belong to the same cluster (then cluster color is used) or to different clusters (then shown in black). The right plot shows their three robustness analysis results when nodes are removed in random (replications are performed for statistic robustness) considering an additional constraint: when testing the robustness of a cluster, nodes belonging to that cluster are not removed (constrained nodes). Dashed vertical lines indicate when only constrained nodes remain non-disrupted. The size of the normalized area under the curve (reported in the top-right corner of right plot) is adopted as an aggregated metric for network robustness, clearly showing that the network remains largely intact as long as either C1 or C2 are not disrupted. (Map is created using Matplotlib and Basemap https://matplotlib.org/basemap/stable/).

random failures from 71% up to 86% and 82% (after controlling for the number of nodes considered). Allowing nodes outside of C3 (which primarily consists of peripheral nodes) to fail contributes to a rapid fragmentation of the network since C3 contains numerous fragmented sub-graphs. While both C1 and C2 share similar features, nodes in C1 ultimately form a single fully connected sub-graph, for which reason we refer to as the primary sub-graph, while approximately only half of the nodes in C2 are connected in a single sub-graph (located in the central northern part of Europe).

Criticality analysis for a multi-modal multi-layer network

The two long-distance transportation networks of rail and air could potentially be considered in a single multi-modal network given the common set of nodes and their two unique sets of edges. The integration of the two networks could potentially offer robustness advantages by increasing network redundancy, i.e. travellers may travel by rail in the event that their air connection is disrupted for (parts of) their journey. We are specifically interested in the contribution of the rail network for improved robustness in the event of disruptions in the air network. While the European rail network does allow in principle for travelling between any origin and any destination in the absence of air connections, travelling by train often requires performing more transfers, i.e. interchanging at the stations. To this end, we measure for each node its connectivity level when its air links are disrupted, calling *air connectivity dependency* ρ_i and plot it in Fig. 6. Unlike previous analyses, nodes remain connected while all air edges connecting to a single node are disrupted at a time. Darker nodes in Fig. 6 (left) indicate higher ρ_i values, meaning strong dependence on air connections and thereby a limited added robustness value offered by rail connections. Consequently, darker nodes are significantly impacted by disruptions in the air network, despite the presence of rail connections. Nodes with highest values of ρ_i are Barcelona (ES), Rome (IT), and London (UK); nodes with lowest values are Košice (SK), Bergen (NO), and Ankara (TR). Cities located in North-Western Europe (the Netherlands, Belgium, and Western parts of Germany) form a homogeneous cluster with high values of ρ_i. The reason is that these cities occupy central positions in the air network, resulting in redundancy in air links. As a result, traveling to or from these cities now requires nearly twice as many trip legs. However, disruptions affecting any node in this cluster are mitigated within the cluster itself, as neighboring nodes can act as necessary bridges, thus increasing the likelihood of being travelled along the shortest paths.

Discussion

The robustness of the European rail and air network was assessed through the successive removal of nodes simulating random failures and targeted attacks. Once a node has been attacked and cannot be restored, the network reaches a new configuration, and the process is repeated until only one node remains. We studied L, the size of the largest connected component, to access the robustness of the networks against the fraction of removed

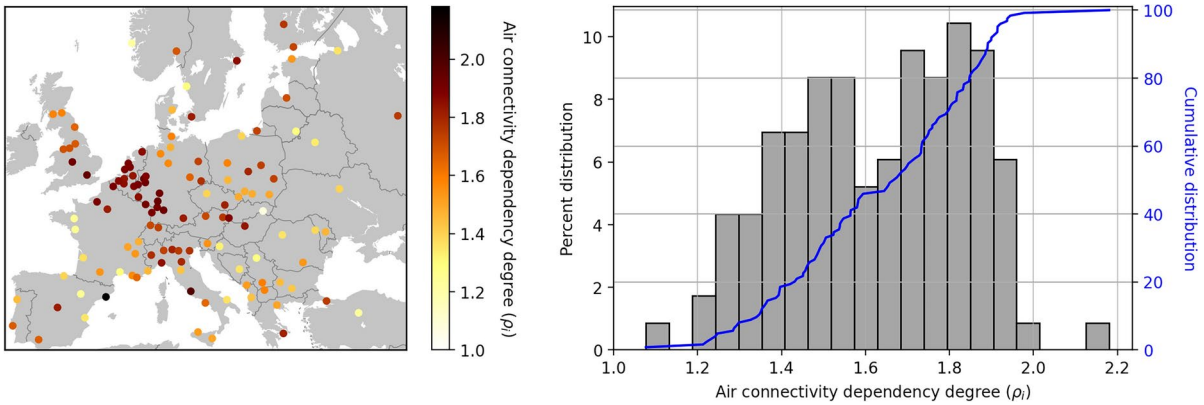

Fig. 6. Distribution of air connectivity dependency degree ρ_i in the multi-modal European network in geographical (left) and histogram (right) plots. The air connectivity dependency is a relative value that represents the multiplier for node *i* of the average number of trip legs needed to reach all other nodes in the network when air routes to or from node *i* are not available, compared to when they are available. Nodes with values close to unity are less dependent to air edges, i.e. rail connections are as important as their air counterparts, and multi-modal trips are likely to happen. Approximately 70% of the nodes have a value of ρ_i equal to or greater than 1.5. (Map is created using Matplotlib and Basemap https://matplotlib.org/basemap/stable/).

nodes. While selecting nodes through targeted attacks resulted in a considerably more rapid degradation than random failures for both networks, the performance of the air network (*I*) does not worsen by more than 10% under any of the scenarios compared with a 71% performance loss for the rail network in the event of removing nodes based on their betweenness centrality values. The results of the random removal strategy indicate that the rail network is particularly sensitive to the specific sequence of node failures, suggesting that path dependency plays an important role in determining network degradation level - i.e., the magnitude of damage of each node depends on the previous attacks. This finding highlights the need to introduce new statistically defined metrics to evaluate the role of nodes beyond path dependency and the presence of resilient sub-graphs.

The rail network is characterised by a lower average node degree compared to the air network - mean node degree is 82 for air nodes compared to only 4 for rail nodes (see Fig. 8). This stems from the fundamental difference in the underlying economics - introducing new edges in the rail network involves next to operational costs high infrastructure investment costs, whereas in the case of air this implies merely operational costs. The lower density of the rail network as compared to the air network - 20 times fewer edges for the same set of nodes - also means that fewer nodes are on the shortest path connecting many origin-destination pairs. Consequently, the rail network is characterised by a more uneven distribution of betweenness centrality values - standard deviation for node betweenness centrality for rail network is 25 times greater than for air network. The robustness analysis shows that a network with numerous connections (high node degree values) is more robust, while a network where betweenness centrality is more unevenly distributed is less robust, particularly towards targeted failures.

Following the rail and air network robustness analysis, we conducted a comprehensive analysis of node criticality. Given its significantly lower robustness and the larger variety in the role of different nodes, we focused on the rail network in our analysis of node criticality. The initial analysis focused on revealing the impact of each node's failure on the extent to which it leads to disconnecting other nodes. We found that approximately 40% of network's nodes have been identified as connecting nodes (i.e., disrupting one of them causes the disconnection of additional nodes) highlighting their criticality. Next, we turned into measuring node criticality within clusters (i.e., in collaboration with other nodes). We utilized the mean profile of node betweenness against x to generate a signature per node and then used this as input for identifying three distinct clusters (obtained by clustering algorithm) of nodes. The results unravel clusters which share common behavior in the event of network disruptions. This analysis helps us better grasp the rail network's fragility. Lastly, we considered the case of a multi-modal graph, aiming to quantify node dependency on air edges in the presence of both air and rail connections. Our findings revealed a cluster of nodes highly dependent on air connections, concentrated in the North-Center region of Europe where air edges are more dense. The primary sub-graph of C1 is comprised of a small sub-set of cities (about 14% of the network nodes) yet is directly connected to almost 48% of network nodes. There is thus a bridge connecting almost half of the network through the sub-network of this compact cluster which our analysis identified. Policy makers can leverage our findings by for instance enhancing inter-cluster connections to prevent peripheral nodes from becoming isolated or improve air dependency as a strategy to withstand potential failures in the rail and multi-modal network connectivity.

The results of our analysis highlight that some nodes/cities are highly dependent on the rail transport network. Specifically, cities with a low air connectivity dependency degree (for which the metric approaches 1) are characterised by having many origin-destination pairs that can only be reached by means of multi-modal journeys (e.g., train to a hub and then by air). A disruption of the railway infrastructure is therefore particularly damaging for the connectivity of these cities. It is hence recommended to strengthen the railway infrastructure

at these nodes to mitigate the risk of significant disruptions in multi-modal connectivity by addressing both of failure probability and the impact of a failure once it occurs. Related measures include maintenance schemes, deploying switches, local capacity enhancements, and air-rail integration and alliance programs.

Results from both the single and clustered analyses of node criticality indicate a resilient structure of interconnected nodes. Decision makers can leverage these findings to develop effective strategies for protecting critical nodes and reinforcing their connections within the network. The clustered analysis, in particular, has highlighted the existence of multiple sub-graphs in our multi-layer network. Within the compact primary sub-graph of C1, strong intra-cluster connections are essential for bolstering the network's robustness. Consequently, inter-cluster connections can be strategically managed through air and rail traffic control to ensure network continuity, even for those nodes likely to be isolated. The multi-modal analysis has been especially valuable in identifying regions, such as Southeastern Europe, where many nodes exhibit low dependence on air transport. This finding suggests that these regions are particularly vulnerable to rail transport disruptions, emphasizing the importance of key nodes whose performance has far-reaching effects on the network.

In summary, our findings reveal: (1) a strong correlation between network structure and its robustness against both targeted and random node attacks; (2) European rail nodes serve different roles based on their position and topological properties; (3) a hierarchical order exists within the rail network, as demonstrated by statistical metrics; (4) a primary sub-graph of nodes has been identified, whose protection from attacks can greatly enhance network's overall robustness; (5) additional sub-graphs have been identified, and their preservation can be ensured by strengthening their connections with the primary sub-graph; and (6) improving air dependency as a strategy to withstand potential failures.

Future research may expand on our analysis by accounting for temporal aspects of the air and rail transport services. Representing service networks using time-dependent graphs where each link corresponds to a specific train or plane departure will allow for the consideration of various service disruption duration. Alternatively, future work may incorporate information about service frequencies by utilising a labeled version of the Service-space graph (see an example from the urban public transport context in[29]). Such a representation will allow investigating the impacts of partial failures and thereby establishing whether the vulnerability curve as defined in[30] is linear, convex or concave for different network elements and the consequences thereof for prioritising mitigation measures.

Another direction in which the graph representation can be enhanced is by considering passenger demand. The inclusion of passenger flows would enable quantifying the share of unsatisfied demand - which is closely related to the network indicator of the size of the largest connected component - and the impacts of disruptions on passenger flow distribution. We also note that our analysis is limited to intra-European travel. The consideration of trans-continental flights will allow analyzing the impacts of various disruptions on the consolidation of flows for connecting flights at key gateways. Finally, one may broaden the analysis prism from network vulnerability to network recoverability by considering the respective recovery strategies[31].

Methods

Robustness analysis and indicators

The iterative node removal procedure requires as input a directed graph $G(N, E)$ and a node selection strategy σ. It operates with index k ranging from 0 to $|N| - 1$, successively removing nodes. In the following we assume that the failure is complete and lasting. In other words, the failure is of the highest severity with the node in question and all connecting links becoming dysfunctional. Furthermore, once a node fails it remains dysfunctional and does not recover within the analysis period.

Any sequence of failed nodes is an ordered list with k entries, denoted as $s^{(k)} \in N^{(k)}$, such that $N^{(k+1)} \equiv N^{(k)} \setminus s^{(k)}$, representing the removed node at stage $k+1$. The relationship between index k and x is expressed in Eq. 1

$$x^{(k)} = \frac{|N^{(k)}| - |N|}{|N|} = \frac{k}{|N|}, \quad \forall\, k = 0 \ldots, |N| - 1 \tag{1}$$

where $|N^{(k)}| = |N| - k$ as k nodes have been already removed.

Any strategy σ defines a sequence of disrupted nodes. Strategies of targeted attacks simulate a node disrupted sequence where at each stage k a node is selected as the one that maximizes the assumed strategy (maximization of node degree σ_d or betweenness centrality σ_b). It is important to note that these indicators depend on the stage k, making the sequence not definable a-priori when $k = 0$, but rather subject to re-assessment per stage. They are deterministic, yielding a fixed sequence. Conversely, σ_r is not deterministic and also not dependent on the stage index, identifying each replication as a different sequence of visited nodes. This feature enables the exploration of scenarios where the removal of a node could exert different impacts.

We measure the overall network robustness in withstanding a specific removal strategy by means of the following aggregated metric I computed according to Eq. 2, which is generalized for network robustness with node clusters.

$$I(\sigma) = \sum_{k=0}^{|N|-|C|-1} \frac{L^{(k)}(\sigma)}{|N^{(k)}|} \tag{2}$$

This formulation is the sum over discrete bins of stages, but the integral of $L(x, \sigma)$ curve holds for continuous, equivalently. We compactly denote $L(x^{(k)}) = L^{(k)}$. In our analysis, $L^{(k)}$ refers to the size of the largest connected

component. We choose to adopt this metric because it is (i) always present in a network of non-zero size, (ii) monotonically decreasing, and; (iii) closely related to the reduction in the share of services and acts as a proxy of the share of unsatisfied demand.

The critical node analysis examines $\bar{w}_i$, providing insight into the individual nodes that are found to be most critical in determining network degradation level. For each node, data are organized according to the stage and the replication. The three-dimensional matrix W is defined as follows Eq. 3.

$$W_{ikm} = \begin{cases} L^{(k,m)} - L^{(k+1,m)} & \text{if} \quad i = s^{(k,m)} \\ -1 & \text{otherwise} \end{cases} \qquad \forall i \in N, \quad \forall k = 0 \ldots, |N| - 2, \quad m = 1 \ldots, M \tag{3}$$

Then, the mean node dependency degree is computed by Eq. 4

$$\bar{w}_i = \frac{1}{q_i} \sum_{m=1}^{M} \sum_{k=0}^{|N|-2} W_{ikm} \quad \forall i \in N \tag{4}$$

where, q_i corresponds to the number of stages wherein node i has a value other than -1, i.e. its removal led to the disconnection of additional nodes (computed over all replications). The metric can be used to analyze the robustness of any network. We applied this analysis to the European air network. The results for the air network showed that all nodes have similar values of $\bar{w}_i$, which are close to unity. This aligns with the robustness analysis where the air network closely followed the ideal upper bound limit.

Similarly, the three-dimension matrix B is defined as Eq. 5. For all replications, and all stages, while node i has not been selected yet, the node betweenness centrality is computed.

$$B_{ikm} = \begin{cases} b_i^{(k,m)} & \text{if} \quad i \in N^{(k,m)} \\ -1 & \text{otherwise} \end{cases} \qquad \forall i \in N, \quad \forall k = 0 \ldots, |N|, \quad m = 1 \ldots, M \tag{5}$$

Then, the mean node betweenness profile is the mean over all replications of node i betweenness at each stage k, see Eq. 6.

$$\bar{b}_i(x) = \left(\frac{1}{q_i} \sum_{m=1}^{M} B_{ikm} \quad \forall\, k = 0 \ldots, |N| \right) \quad \forall i \in N \tag{6}$$

where q_i is the effective number of replication wherein node i is still included the network, i.e. $B_{ikm} \neq -1$. Mean node betweenness profiles are used in the critical analysis of clustered nodes. Clusters are identified using the K-Means algorithm, renowned for its efficiency and effectiveness in data analysis[32].

Finally, the air connectivity dependency values used in the critical node analysis for a multi-modal network are computed according to Eq. 7

$$\rho_i = \frac{n_{\mathrm{Y}}(i)}{n_{\mathrm{MMN}}(i)} \tag{7}$$

where, $n_{\mathrm{Y}}(i)$ and $n_{\mathrm{MMN}}(i)$ are the average number of trips legs with node i as either an origin or a destination when there are no air links connecting to/from this link, or in their presence, respectively.

Data

Data[33] for our analysis have been the directed graphs $G(N, E)$ for both networks. The network's nodes are part of the set N, interconnected through edges belonging to the set E. Notably, the node set is the same for rail and air networks. For the rail network, the graph is constructed so that two nodes are connected (or adjacent) if there is at least one weekly service running on a railway infrastructure segment connecting them; while, in the case of the air network, two nodes are connected if there is at least one flight per week between node i and j. Figure 7 shows graphs of the European rail, air, and combined network. At the initial stage, networks are fully connected $L^{(0)} = |N|$.

Moreover, the distributions of node centrality indicators are displayed in Fig. 8. Given the much higher number of edges in the air network, the mean node degree is also considerably higher in the air network. Moreover, due to the abundance of connections, none of the nodes needs to be traversed by a large share of the shortest paths, as indicated by the lower value of node betweenness.

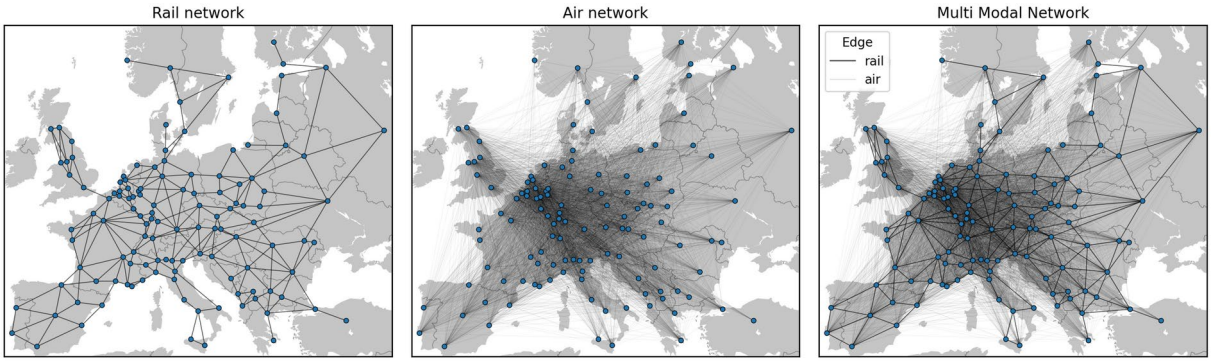

Fig. 7. Representation of studied networks. From right to left: Rail, Air, and Multi-Modal. Nodes, depicted as blue dots, represent a set of 124 main metropolitan areas spanning 34 countries which have been selected based on population size and significance (e.g., capital cities). The set of nodes is identical for all networks. The rail network consists of 257 edges. The air network is composed of 5173 edges. The inclusion of an edge implies the presence of at least a weekly service traversing this edge. The multi-modal network has a total of 5430 links, providing a comprehensive view on how considered metropolitan areas are connected through both rail and air transportation networks. (Maps are created using Matplotlib and Basemap https://matplotlib.org/basemap/stable/).

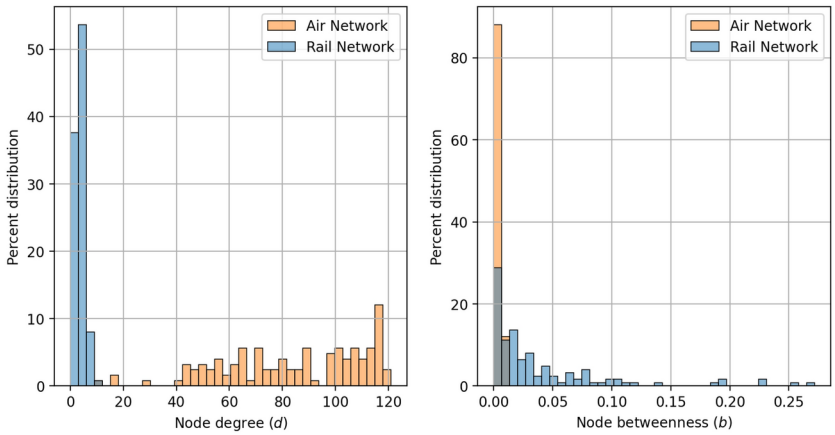

Fig. 8. Distribution of node topological indicators for the European rail and air networks. Node degree (left) represents, for each node, the number of directly connected nodes. In the case of rail, almost 55% of the nodes have a degree around 3. For air, in contrast, nodes with higher degrees are likely, ranging from 12 for Kosice (SK) to 121 for London (UK). Node betweenness, representing the share of shortest paths from any origin to any destination that traverses a specific node, is shown on the right. The highest betweenness value is 0.34 for Wien (AT), indicating that 34% of routes in the network pass through that node. The air network has a smaller range and lower values. Almost 90% of air nodes have a coefficient nearly equal to 0. suggesting a high level of redundancy.

Data availability

The data underlying this analysis is available via a public repository: https://data.4tu.nl/datasets/2627470d-7184-4f21-bc01-80bbf0ce211c/1. The datasets generated during and/or analysed during the current study are available from the corresponding author on reasonable request.

Received: 4 April 2024; Accepted: 11 October 2024
Published online: 06 November 2024

References

1. Nicholson, A. & Du, Z.-P. Degradable transportation systems: An integrated equilibrium model. *Trans. Res. Part B: Methodol.* **31**, 209–223 (1997).
2. Berdica, K. An introduction to road vulnerability: What has been done, is done and should be done. *Trans. Policy* **9**, 117–127 (2002).
3. Faturechi, R. & Miller-Hooks, E. Measuring the performance of transportation infrastructure systems in disasters: A comprehensive review. *J. Infrastruct. Syst.* **21**, 04014025. https://doi.org/10.1061/(ASCE)IS.1943-555X.0000212 (2015).
4. Mattsson, L.-G. & Jenelius, E. Vulnerability and resilience of transport systems - A discussion of recent research. *Trans. Res. Part A: Policy Pract.* **81**, 16–34 (2015).
5. Bell, M. G. & Cassir, C. Risk-averse user equilibrium traffic assignment: An application of game theory. *Trans. Res. Part B: Method.* **36**, 671–681. https://doi.org/10.1016/S0191-2615(01)00022-4 (2002).
6. Bell, M. G., Kanturska, U., Schmöcker, J. D. & Fonzone, A. Attacker-defender models and road network vulnerability. *Philos. Trans. Royal Soc. A* **366**(1872), 1893–1906 (2008).
7. Jenelius, E. & Mattsson, L.-G. Road network vulnerability analysis of area-covering disruptions: A grid-based approach with case study. *Trans. Res. Part A: Policy Pract.* **46**, 746–760. https://doi.org/10.1016/j.tra.2012.02.003 (2012).
8. Scott, D. M., Novak, D. C., Aultman-Hall, L. & Guo, F. Network robustness index: A new method for identifying critical links and evaluating the performance of transportation networks. *J. Trans. Geogr.* **14**, 215–227. https://doi.org/10.1016/j.jtrangeo.2005.10.003 (2006).
9. Jenelius, E., Petersen, T. & Mattsson, L.-G. Importance and exposure in road network vulnerability analysis. *Trans. Res. Part A: Policy Pract.* **40**, 537–560. https://doi.org/10.1016/j.tra.2005.11.003 (2006).
10. Chen, A., Yang, C., Kongsomsaksakul, S. & Lee, M. Network-based accessibility measures for vulnerability analysis of degradable transportation networks. *Netw. Spatial Econom.* **7**, 241–256 (2007).
11. James Sullivan, L.A.-H. & Novak, D. A review of current practice in network disruption analysis and an assessment of the ability to account for isolating links in transportation networks. *Trans. Lett* **1**, 271–280. https://doi.org/10.3328/TL.2009.01.04.271-280 (2009).
12. Cats, O. The robustness value of public transport development plans. *J. Trans. Geogr.* **51**, 236–246 (2016).
13. Lordan, O., Sallan, J. M. & Simo, P. Study of the topology and robustness of airline route networks from the complex network approach: A survey and research agenda. *J. Trans. Geogr.* **37**, 112–120 (2014).
14. Pien, K.-C., Han, K., Shang, W., Majumdar, A. & Ochieng, W. Robustness analysis of the European air traffic network. *Trans. A: Trans. Sci.* **11**, 772–792 (2015).
15. Zhou, Y., Wang, J. & Huang, G. Q. Efficiency and robustness of weighted air transport networks. *Trans. Res. Part E: Log. Trans. Rev.* **122**, 14–26 (2019).
16. Lin, J. & Ban, Y. The evolving network structure of us airline system during 1990–2010. *Phys. A: Stat. Mech. Appl.* **410**, 302–312 (2014).
17. Verma, T., Araújo, N. A. M. & Herrmann, H. J. Revealing the structure of the world airline network. *Sci. Rep.* **4**, 5638 (2014).
18. Wei, S. et al. Hierarchical structure in the world's largest high-speed rail network. *PloS one* **14**, e0211052 (2019).
19. Cao, W., Feng, X. & Zhang, H. The structural and spatial properties of the high-speed railway network in China: A complex network perspective. *J. Rail Trans. Plan. Manage.* **9**, 46–56 (2019).
20. Jiao, J., Zhang, F. & Liu, J. A spatiotemporal analysis of the robustness of high-speed rail network in China. *Trans. Res. Part D: Trans. Environ.* **89**, 102584 (2020).
21. Li, T. & Rong, L. Spatiotemporally complementary effect of high-speed rail network on robustness of aviation network. *Trans. Res. Part A: Policy Pract.* **155**, 95–114 (2022).
22. Gao, Y., Liang, C., Zhou, J. & Chen, S. Robustness optimization of aviation-high-speed rail coupling network. *Phys. A: Stat. Mech. Appl.* **610**, 128406 (2023).
23. Wang, Z. et al. Recent advances in modeling the vulnerability of transportation networks. *J. Infrastruct. Syst.* **21**, 06014002. https://doi.org/10.1061/(ASCE)IS.1943-555X.0000232 (2015).
24. Berche, B., von Ferber, C., Holovatch, T. & Holovatch, Y. Resilience of public transport networks against attacks. *The European Physical Journal B* (2009).
25. Cats, O. & Krishnakumari, P. Metropolitan rail network robustness. *Phys. A: Stat. Mech. Appl.* **549**, 124317 (2020).
26. Liu, J., Zhou, M., Wang, S. & Liu, P. A comparative study of network robustness measures. *Front. Comput. Sci.* **11**, 568–584 (2017).
27. Albert, R., Jeong, H. & Barabási, A.-L. Error and attack tolerance of complex networks. *Nature* **406**, 378–382 (2000).
28. Dowling, R., Skabardonis, A., Alexiadis, V. *et al.* Traffic analysis toolbox, volume iii: Guidelines for applying traffic microsimulation modeling software. Tech. Rep., United States. Federal Highway Administration. Office of Operations (2004).
29. Luo, D., Cats, O., van Lint, H. & Currie, G. Integrating network science and public transport accessibility analysis for comparative assessment. *J. Trans. Geogr.* **80**, 102505 (2019).
30. Cats, O. & Jenelius, E. Beyond a complete failure: the impact of partial capacity degradation on public transport network vulnerability. *Trans. B: Trans. Dyn.* **6**, 77–96 (2018).
31. Massobrio, R. & Cats, O. Topological assessment of recoverability in public transport networks. *Commun. Phys.* **7**, 108 (2024).
32. Mohri, M., Rostamizadeh, A. & Talwalkar, A. *Foundations of machine learning* (MIT Press, 2018).
33. Tanner, S., Cats, O., Provoost, J. & Corman, F. Tradable mobility credits for long-distance travel in europe - impacts on the modal split between air, rail and car. https://doi.org/10.3929/ethz-b-000607296 (2023).

Acknowledgements

N.I. acknowledges Sapienza University of Rome for the doctoral student mobility grant 2022 and both authors are grateful for Prof. Guido Gentile for making this collaboration possible and for his remarks on the submitted manuscript.

Author contributions

Conceptualisation: O.C.; Methodology, Investigation, Writing - Original Draft, Writing - Review and Editing: O.C. and N.I.; Software and Formal analysis: N.I.

Competing interests

The authors declare no competing interests.

Additional information

Correspondence and requests for materials should be addressed to O.C.

Reprints and permissions information is available at www.nature.com/reprints.

Publisher's note Springer Nature remains neutral with regard to jurisdictional claims in published maps and institutional affiliations.